Research Journal of Pharmaceutical, Biological and Chemical Sciences

Investigation in Electrochemical Impedance Spectroscopy and Energy Dispersive Analysis of X-rays Measurements of Nanoilmenite/amorphous silica Composite Coating for Steel Petroleum Structures in Oil-wells Formation Water in the term of Cold Galvanizing Technology.

A.M. Al-Sabagh [1], M.I. Abdou [1], M.A. Migahed [1], A.M. Fadl [1,*], M.F. El- Shahat [2]

[1] Egyptian petroleum Research Institute (EPRI), Nasr city, Cairo, Egypt,
[2] Ain Shams University, Chemistry Department, Faculty of Science, Cairo, Egypt

ABSTRACT

The present work was performed to investigate the corrosion protection behavior of some alkyd-based cold galvanizing coating formulations containing different dispersed amounts of novel fabricated nanoilmenite/amorphous silica composite (NI/AS) particles applied on the carbon steel surface. TEM photograph demonstrated that the prepared nanocomposite particles were of a lamellar shape and the average diameter of the particles is 20 nm. SEM micrographs illustrated the flaky-like nature of NI/AS and spherical shape of Zn-dust particles. The corrosion protection behavior of the nano composite modified coated films in oil-wells formation water solution has been investigated by the electrochemical impedance spectroscopy (EIS) technique. The EIS results ensured that the excellent corrosion protection effect was due to the highly-dispersion of NI/AS particles had a lamellar flaky-like shape with a shield of overlapping plates in which increased the interface surface interaction between these nanoparticles and the resin matrix and led to occupying any holidays through the coating film. Energy dispersive analysis of X-rays (EDX) technique was utilized to survey the corrosion inhibition effect of the protective nanocomposite cold galvanizing coated film formed on the steel surface in the formation water solution. The obtained results offered advanced corrosion protection properties of the NI/AS modified cold galvanizing coating.

Keywords: Nanoilmenite/amorphous silica Composite Particles, Amorphous Silica; Electrochemical Impedance, Protection Efficiency and EDX.

*Corresponding author

INTRODUCTION

The application [1] of zinc rich paints (ZRP) on ferrous substrates is a very efficient approach of anticorrosion protection. They are utilized in different aggressive media such as sea water, marine and industrial environments. For solvent based zinc rich paints, zinc particles provide cathodic protection at least in case of the beginning of immersion in which a galvanic coupling is created between zinc particles and the metal substrates and it can dissolve then, act as sacrificial pigment. [2, 3]. Then, a long term protection develops due to the formation of zinc corrosion products, supporting the barrier effect of the paint [4]. The metallic Zn-dust content in the dry film is a very significant parameter to be confirmed in the technical specifications of zinc rich paints. The corrosion protection behavior of solvent based zinc rich paints rely strongly on pigment volume concentration (PVC), shape and size of zinc particles. For example, Pereira et al. [5] proved that the chemical nature of the vehicle and the zinc particle size are also very important. The Zn-dust particles (spherical or lamellar shape, or a combination of both shape) are dispersed in an inorganic (usually orthosilicates) or organic binder (usually epoxies) [6]. Ilmenite is a non-toxic pigment contains titanium-iron oxide mineral with the idealized formula ($FeTiO_3$). It is a weak magnetic black or steel-gray solid. Ilmenite is the most important ore of titanium dioxide pigment. Egyptian ilmenite ore was utilized after grinding to micro-sized scale and processing as anticorrosive pigment and mechanical property promoter for epoxy coating formulation technology [7].

Nanocomposite is a multiphase solid material where one of the phases has one, two or three dimensions of less than 100 nm [8]. The solid phase can be amorphous, semi-crystalline, grain or a combination. The solid phase can also be organic, inorganic, or a combination. The mechanical, thermal, optical and electrochemical properties of the nanocomposite will vary markedly from that of the component materials. A large number of studies dedicated to coating systems containing nanofillers have already been published such as on epoxy/TiO2, Latex/silica [9, 10] and these studies show that compared to conventional organic coatings containing microfillers, the use of nanofillers has advantages such as improvement in scratch, abrasion, heat, radiation and swelling resistance and decrease in water permeability and increase in hardness, wetherability, modulus. To make a successful 'nanoorganic coating' it is imperative to disperse the nanoparticles through the binder. If this is not achieved, agglomerates will form and the expected properties will not be obtained.

The present work aims to prepare nanoilmenite/amorphous silica composite particles and evaluate its corrosion protection behavior on the carbon steel surface when added with different concentrations to cold galvanizing coating. Also, to study the surface morphology of these modified cold galvanizing coated films against uncoated blank carbon steel in formation water solution was made by using EDX investigation.

EXPERIMENTAL

Materials

Chemicals

Alkyd resin 60% and Benton were conducted from Chemical Partners Company. Zn-dust pigment was acquired from WL Company for Paints and Chemicals. White sand, potassium and sodium feldspars, calcium carbonate, boron, zinc, aluminium and zirconium oxides were obtained from ARKAN Company for Industry and Mining. BYK-066 N (polysiloxanes), was obtained from BYK-Chemie USA Inc. Xylene, ethylene glycol, n- butyl glycol were gained from El-Mohandes Company for Chemicals and Trading and were used in technical grades.

Egyptian ilmenite ore ($FeTiO_3$, iron titanium oxide pigment)

A great deposit of Egypt occurs in Wadi Abu Ghalaga in the South Eastern Desert. Ilmenite was anatomized by Thermo ARL ADVANT XP-385 XRF model and its physicochemical characteristics are depicted in **Tables 1 and 2.**

Table 1: Characterization of Ilmenite Ore

Character	Color	Bulk density (g/cm³)	Specific gravity	Mohs Scale of hardness	Luster	Oil absorption gm/100gm	Refractive Index
Result	Black	2.2	4.45	6-6.5	Metallic	8	2.94

Table 2: XRF Analysis of Ilmenite Ore.

Element	Fe$_2$O3	TiO$_2$	SiO$_2$	MgO	Al$_2$O$_3$	CaO	ZnO	MnO	V$_2$O$_5$	Cr$_2$O$_3$	ZrO$_2$
Result (%)	49.78	33.76	6.94	4.79	2.96	0.79	0.29	0.25	0.24	0.11	0.09

Preparation of the carbon steel samples and its composition

The carbon steel samples used in the present study were divided into specimens with dimensions of 1cm x 1cm x 0.8 mm for EDX and the EIS investigations. The specimens were mechanically prepared with emery paper up to 80 (medium grade). Then, it was washed in acetone and double distilled water before immersion in the test solution and its chemical composition is offered in **Table 3.**

Table 3: Chemical Composition of Testing Carbon Steel.

Element	C	Si	Mn	P	S	Ni	Al	Fe
Content (%)	0.13	0.23	1.26	0.017	0.012	0.063	0.013	Bal 98.275

Test solution

The test solution in this study was the connected formation water during crude oil production handed over from Qarun Petroleum Company (QPC), Egypt. The chemical composition of this water has been performed using ionic chromatography as shown in Table 4.The specific gravity of this water was 1.109, PH (6.23), The salinity as NaCl (151,581ppm,wt), The total alkalinity (350ppm,wt) and the total hardness (19.321).

Table 4: Chemical Composition of Oil-wells Formation Water

Ionic concentration	Na$^+$ and K$^+$	Ca^{2+}	Mg^{2+}	Ba^{2+}	Sr^{2+}	Cl$^-$	SO$_4^{-2}$	HCO$_3^-$	T.D.S
Conc, ppm(w/w)	56,439	31,000	2700	350	85	230,000	350	85	230,000

Methods and techniques

Preparation of ilmenite nanoparticles [FeTiO$_3$ (NPs)]

The ilmenite nanoparticles were processed by ball milling method. The planetary ball mill PM 200-RETSCH-short grinding times was utilized to grind 20µm size of ilmenite powder for 12h in an automatic grinding chamber with two grinding stations to get the highest degree of ilmenite fineness around 0-20 nm size range.

Synthesis of amorphous silica composite particles

Amorphous silica particles were synthesized by mixing 70.5% by weight of Egyptian white sand (source of SiO$_2$), 3% potassium feldspar (source of K$_2$O), 1.14% sodium feldspar (source of Na$_2$O), 6.9% calcium carbonate (source of CaO), 0.5% boron oxide (B$_2$O$_3$), 0.3% zinc oxide (ZnO), 17.1% aluminum oxide (Al$_2$O$_3$) and 0.5% zirconium oxide (ZrO$_2$) after grinding process to reach 1-75µm size powder range for 20 min in a collection column. Heat treatment (fusion) for the powder mixture at 1350 ^{O}C in ITALO oven was carried out

until a molten liquid was composed then, water quenching operation at temperature 30 ^{O}C was made [11] and grinding the final product to 20µm size powder with specific gravity of 2.78 g/cm^2 and Mohs scale of hardness equal 7.9. XRF analysis of amorphous silica composite was described in **Table 5.**

Table 5: Chemical Composition of Synthesized Amorphous Silica Particles.

Component	SiO_2	TiO_2	Al_2O_3	Fe_2O_3	CaO	Na_2O	MgO	K_2O	ZnO	ZrO_2	B_2O_3
Percent (%)	70	0.01	17.3	0.05	6	1.14	1.2	3	0.3	0.5	0.5

Preparation of nanoilmenite/amorphous silica composite (NI/AS) particles

The nanocomposite (NI/AS) was prepared by mixing 20g of nanoilmenite and 80g of synthesized amorphous silica composite particles as 20:80% by weight homogeneously in a container for 20 min. The mixture formed was added gradually to 40g ethylene glycol and 10g BYK-066 N (polysiloxanes with ingredients as 2,6-dimethyl 4-heptanone and 2-butoxyethanol dissolved in diisobutyl ketone) and stirring by using ultrasonic devices for 45 min till a suspension with homogeneous appearance be formed to establish the nanoilmenite/amorphous silica composite paste**.** Then, the suspension was dried at 70 ^{O}C for 24h**.** After milling, the product is made up of fined black powder [12, 13].

TEM characterization of nanoilmenite/amorphous silica composite (NI/AS)

TEM of the NI/AS particles was conducted at an accelerated voltage of 200 KV electron microscopes (JEM2100 La B6, Japan)**.** In the TEM, the solid samples was dispersed in ethanol solution using ultrasonicator and then dropped on a copper grid coated with carbon film prior to inserting the samples in the TEM column, the grid was vacuum dried for 15 min.

SEM micrographs of nanoilmenite/amorphous silica composite (NI/AS) and Zn-dust particles

SEM micrographs of the NI/AS and Zn-dust particles were clarified by JOEL-5410 scanning electron microscope (Japan) utilized for this investigation. All micrographs of the investigated particles were carried out at magnification of 500 X.

Modification of the coating

Soya bean oil (short oil) alkyd resin was used as coating vehicle for the investigated cold galvanizing coating. The coating formulations with and without the NI/AS modifier are depicted in **Table 6**. The modified nanocomposite coating formulations were prepared by adding the NI/AS particles with different amounts (1.2, 2.4, 3.6, 4.8, 6%) by weight of the total formulation content to the alkyd resin as binder and adding xylene as a thinner with stirring for 30 min by using mixer with ultrasonic devices. Then, the formed suspension was treated with Benton as a viscosity improver, DOP (dioctyl phithalate) as a plasticizer and n-butyl glycol as retardant to the paint and mix for 10 min. Therefore, Zn-dust pigment was added with stirring for 15 min to form five cold galvanizing coating formulations modified with the NI/AS particles (CG-B, CG-C, CG-D, CG-E and CG-F) against another unmodified coating (CG-A). The dispersion and de-agglomeration of solids into liquids is an important implementation of ultrasonic devices.

Table 6: Various Cold Galvanizing Coating Formulations.

Coating code	Short alkyd resin (%)	Xylene (%)	Benton (%)	ENI/AS (%)	Zn-dust (%)	Di octyl phithalate (%)	n-Butyl glycol (%)
CG-A (without ENI/AS modifier)	13	23.5	1.5	-	60	1.5	0.5
CG-B	13	23.5	1.5	1.2	58.8	1.5	0.5
CG-C	13	23.5	1.5	2.4	57.6	1.5	0.5
CG-D	13	23.5	1.5	3.6	56.4	1.5	0.5

| CG-E | 13 | 23.5 | 1.5 | 4.8 | 55.2 | 1.5 | 0.5 |
| CG-F | 13 | 23.5 | 1.5 | 6 | 54 | 1.5 | 0.5 |

Coating thickness

The dry film coating thickness (DFT) on carbon steel panel was measured by Positector 6000(USA) in the gauge from 40 to 45 µm.

Electrochemical impedance spectroscopy

The measurements were conducted using Voltalab 40 Potentiostate PGZ 402 combined with easy corrosion program (Voltamaster 4). A classical three-electrode glass cell, consisting of steel working electrode (WE), a platinum counter electrode (CE) and a saturated calomel electrode (SCE) as reference electrode was utilized for electrochemical measurements. The working electrode was first immersed into the test solution for 90 minutes to set a steady state open circuit potential (E_{ocp}).The EIS diagrams are offered in Nyquist plots in the frequency range from 100 Hz –50 mHz with a 4 mV sine wave as exiting signal at open circuit potential. The EIS spectra from attached films were analyzed using nonlinear least squares fitting (with ZSimWin) to an $R[Q[R[QR]]]$ model circuit as shown in **Fig. 4** [Q= constant phase element]. This is a representative circuit used for coated materials with a conducting path way modeled as a resistance in series with parallel RC combination at metal surface to represent the electrochemical reaction there (or more recently RQ to represent non-ideal behavior). The capacitance (or Q) of the organic coating is ordered in parallel with this combination and short-circuits of the whole combination at high frequency. EIS spectra from coating films which should in outwardly be proportioned $R[C[R [CR]]]$, but were actually analyzed with the circuit $R [Q[R [QR]]]$ as shown in **Fig.4** which yielded a better fit.

Energy dispersive analysis of X-rays (EDX)

EDX system attached with a JOEL 5410 (Japan) scanning electron microscope was used for elemental analysis of chemical characterization of film formed on the steel surfaces. The surface morphology of polished carbon steel specimen blank (without coating film), untreated and treated nanocomposite cold galvanizing coated films were examined after exposure to oil-wells formation water solution. As a type of spectroscopy, it relies on the investigation of sample through interaction between electromagnetic radiation and the matter. So that a detector was used to convert X-ray energy into voltage signals. This information is sent to a pulse processor, which measure the signals and passed them onto an analyzer or data display and analysis. All micrographs (images) of the corroded specimens were performed at magnification of 500 X.

RESULTS AND DISCUSSION

TEM characterization of the NI/AS particles

The structure of prepared NI/AS particles was characterized by transmission electron microscopy (TEM). TEM image of NI/AS particles shows the homogenized surface of material and provide a unique scope to directly visualize nano-particle morphology. **Fig. 1** shows some aggregates of nanoparticles (NPs) and these particles lie already in the 20 nm-size range. The white dashes illustrated beside nano-sized particle values that were written on the TEM image show the actual size of nano-ilmenite particles that are actually could be visually seen in the range of 20 nm-size. TEM image shows also the approximately lamellar shape of the NI/AS particles with flaky-like nature.
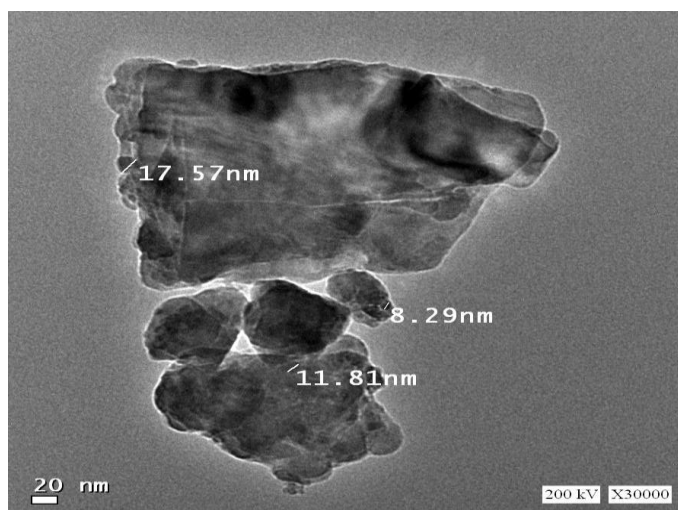
Fig 1: TEM micrograph of the nanoilmenite/amorphous silica composite (NI/AS) particles.

SEM micrographs of the NI/AS and Zn-dust particles

Scanning electron microscopic (SEM) micrographs of NI/AS and Zn-dust particles were illustrated in **Fig. 2.** These clearly show the realistic nature of crystal lattice of the different inorganic pigments used in this study. These characteristic images revealed that, the NI/AS particles had a lamellar flaky-like shape with a shield of the overlapping plates during the highly-dispersion of these particles as shown in **Fig. 2a**. **Fig. 2b** illustrated the approximately spherical shape of Zn-dust particles which permit a clearly-distance between each other during their dispersion through any coating binder.
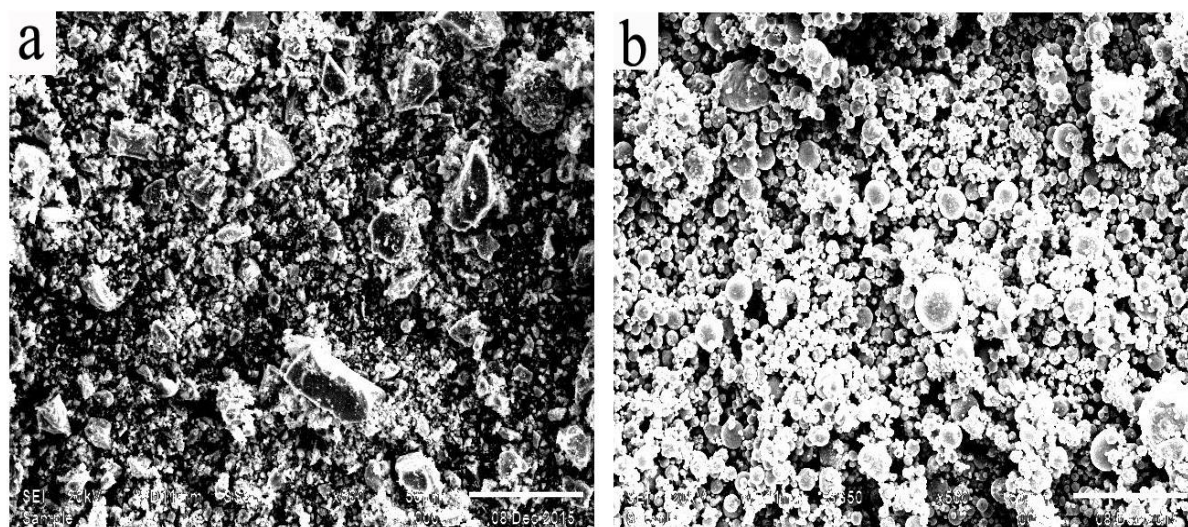
Fig 2: SEM micrographs for (a) lamellar NI/AS particles (b) spherical Zn-dust pigment.

Electrochemical Impedance Spectroscopy (EIS)

The EIS measurements for the cold galvanizing coated steel films have been performed in oil-wells formation water solution. These measurements have been carried out to display the mechanism of the protection function of the modified cold galvanizing coatings on one hand and to ensure the conclusion inferred from dc polarization investigation on the other hand. The Nyquist plots for the cold galvanizing coating formulations are shown in **Fig. 3**. The different curves in **Fig. 3**, arise from the high frequency point which identical to the solution resistance , on the other hand these curves exhibit semicircle shape which revealed that, the rate determining step is the charge transfer one, and its size was increased with increasing the NI/AS concentration.
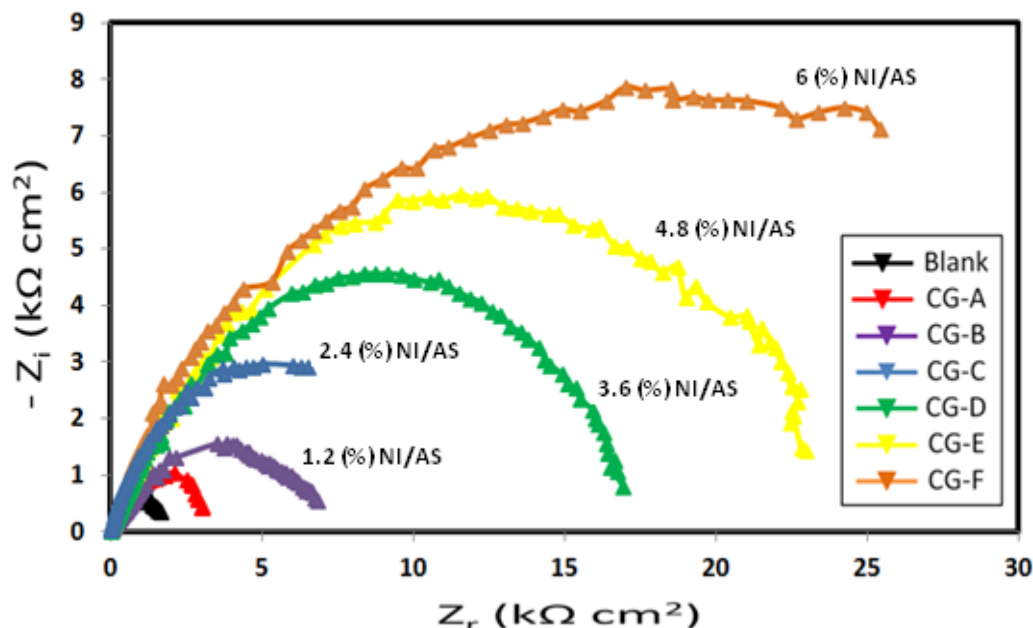
Fig 3: Nyquist plot for various cold galvanizing coated films against blank carbon steel after immersion in oil-wells formation water.

This result compact with the conclusion originated from the studied dc polarization, through the formed coating owns high impedance with increasing the NI/AS loading level in the coating layer. This behavior is owing to an increase in the thickness of the barrier layer; hence it increased the diameter of the semicircle of the impedance plots. Impedance is totally complex resistance when a current transfers through a circuit made of the capacitors, resistors, or insulators, or any combination of these [14]. The Nyquist plots taken out for the investigated cold galvanizing coated carbon steel films offered general performance where the double layer interface of metal / solution does not behave as an ideal capacitor. The diameter of circuit loop increased with increasing the amount of NI/AS particles dispersed with the Zn-dust pigment through the vehicle as illustrated in coating formulations depicted in **Table 6**. It was noted that, with increasing the zinc content (%) by weight in the coating formulation, the circuit loop diameter decreased due to establishing a well electrical conduction within the coating [15]. So, CG-F coating exhibited the largest loop diameter and CG-A coating gave the lowest one. This resulted from a shield of the overlapping plates produced by the NI/AS particles.

To recognize the mechanisms of the corrosive processes, which happen at the surface of the studied films, the fitting of the experimental impedance spectra were applied using the appropriate equivalent electric circuits (EECs). In this study the constant phase element (CPE) was used in the equivalent circuits instead of the ideal electrical capacitance. This element is better characterizing the behavior of the coatings having heterogeneities of the meso-structure and/ or for the chemical composition. The electrochemical behavior of the investigated cold galvanizing coating formulations is well represented by the EEC with two series parallel R-CPE circuits as shown in **Fig. 4**, describing the behavior of NI/AS coating in whole. It is known that, the R_e is the electrolyte resistance nearby the coating film, R_p is the coating pore resistance, Q_c and n_1, respectively, represent the magnitude and exponent of the constant phase element (CPE) of the NI/AS coating. Q_{dl} and n_2 represent the magnitude and exponent of the constant phase element (CPE) of the double layer, which reflect states of the electrochemical reactions under coating.
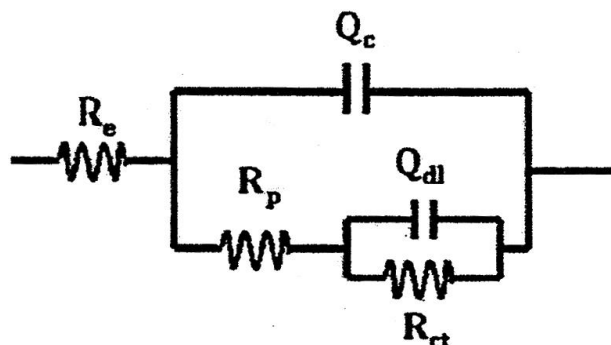
Fig 4: the suggested model for the equivalent circuit of the coating systems in oil-wells formation water for various cold galvanizing coated films against blank carbon steel.

The R_p of the coated steel films can be used to estimate the relative pinholes through the coating matrix. It could be speculated that the measured R_p was characteristic to the coating-electrolyte interface inside the coating (indicating coating porosity/compactness). The protective mechanism of the nanocomposite modified cold galvanizing coated film as shown in **Fig. 5** was summarized as follows. The superior corrosion resistance offered by the combined effect of adsorptions of π- electrons of the aromatic ring and lone pair of oxygen atoms of the physically drying modified alkyd resin which form a coherent plastic film and increase the adhesion forces between the metal surface and the paint, hence reduces the transfer of the corrosive species to metal surface by forming a protective layer over the surface metal. Sacrificial means by using a sacrificial anode such as zinc dust particles in which offer cathodic protection and arise a reduction in the galvanic action of the cold galvanizing paints with time. The zinc layer dispersed on the modified alkyd binder could be degraded when exposed to the aggressive formation water medium without blocking the permeability pathways within the binder as studied in the protection mechanisms of various inorganic and organic zinc rich coatings [16, 17].
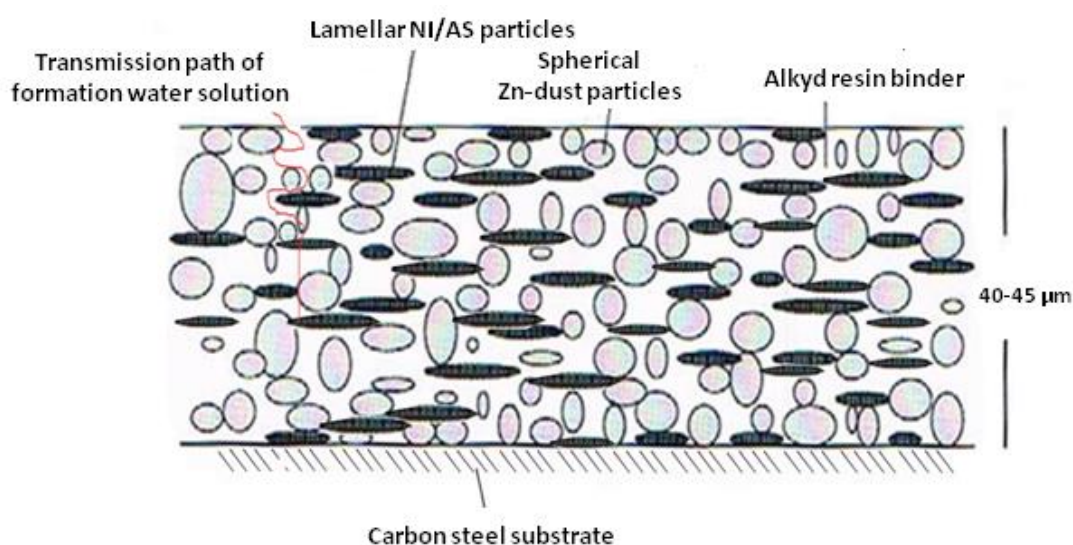

Fig 5: The suggested model for protection mechanism of NI/AS cold galvanizing coating.

Finally, the barrier effect of the nanoilmenite/amorphous silica composite modified cold galvanizing coating films could be attributed to the presence of flaky- like NI/AS particles which aligned parallel to the steel surface through the modified alkyd binder producing a shield of the overlapping plates. This alignment enhanced protection by providing a protective barrier, increasing the film reinforcement and enhancing the inter-coat adhesion. Barrier effect observed from coating films as shown in **Fig. 2** was attributed to the lamellar particles nature of NI/AS in which a physical barrier is formed that prevents the ingress of water, oxygen and ions to inhibit corrosion of the steel and degradation of the binder [18]. It could be noted that, the corrosion products increase

The impedance of this element (Z_{CPE}) is given according to the following equation [19, 20]:

$$Z_{CPE} = \frac{1}{Q_{O\,(j\omega)^n}}$$ (1)

Where the coefficient Q (proportional to the capacitance of the corroding system) is a combination of properties related to different physical phenomena like surface in homogeneousness resulting from surface roughness, electro-active species, inhibitor adsorption, porous layer formation, etc., j is an imaginary number ($j2 = -1$), ω is the angular frequency ($\omega = 2\pi f$) and the exponent n represents a phase shift (its value between −1 and 1). A value of −1 is a characteristic for an inductance, a value 1 corresponds to a resistor, and a value of 0.5 can be assigned to the diffusion phenomenon. The measured values of the impedance parameters inferred from the Nyquist plots using the selected equivalent circuit model as shown in **Fig. 4** are given in **Table 7**.

Sample	R_{ct} (kΩ cm²)	Q_{dl} (μΩ⁻¹ sⁿ cm⁻²)	R_P (kΩ cm²)	n_1	n_2	Q_c (μΩ⁻¹ sⁿ cm⁻²)	R_e (kΩ cm²)	η%
Blank	1.27	311	2.38	0.75	0.63	107.14	0.015	-
CG-A	5.78	1.43	12.30	0.54	0.65	39.2	0.125	78
CG-B	6.97	0.91	14.25	0.71	0.59	15.45	0.283	81.7
CG-C	15.16	0.64	20.25	0.51	0.81	7.34	0.342	91.8
CG-D	17.51	0.66	22.97	0.54	0.85	1.78	0.394	92.7
CG-E	24.08	0.41	28.44	0.63	0.61	0.11	0.453	94.7
CG-F	48.96	0.36	33.19	0.57	0.59	0.02	0.484	97.4

Table 7: EIS Parameters for Uncoated Blank Carbon Steel and Various Cold Galvanizing Coated Films in Oil-wells Formation Water Solution.

Moreover, that the calculated impedance values increased with increasing the NI/AS modifier concentration, this behavior can be visualized quantitatively from the increase of the charge transfer resistance (R_{ct}) with increasing the mass (%) by weight of the modifier in the coating formulation as shown in **Fig. 6**. The increase in R_{ct} can be assigned to the decrease in the number of the active sites (pinholes) spread through the coating surface and then made a decrease in the exposed area to the aggressive medium. Charge transfer resistance was characterized to the steel-electrolyte interface. The impedance parameters which were derived from these figures are listed in **Table 7**. In case of EIS measurements the protection efficiency (η) was calculated by the charge transfer resistance according to the following equation [21–23]:

$$\eta = \left(\frac{R_{ct} - R^\upsilon{}_{ct}}{R_{ct}} \right) \times 100$$ (2)

Where $R^o{}_{ct}$ and R_{ct} are the charge transfer resistance values of unmodified and the NI/AS modified coated films, respectively.

The data in **Table 7** demonstrated that, the protection efficiency increases with increasing the NI/AS modifier amount dispersed in the coating film as shown in **Fig. 7.** The protection efficiency (η) of the tested coatings was increased in the following order:

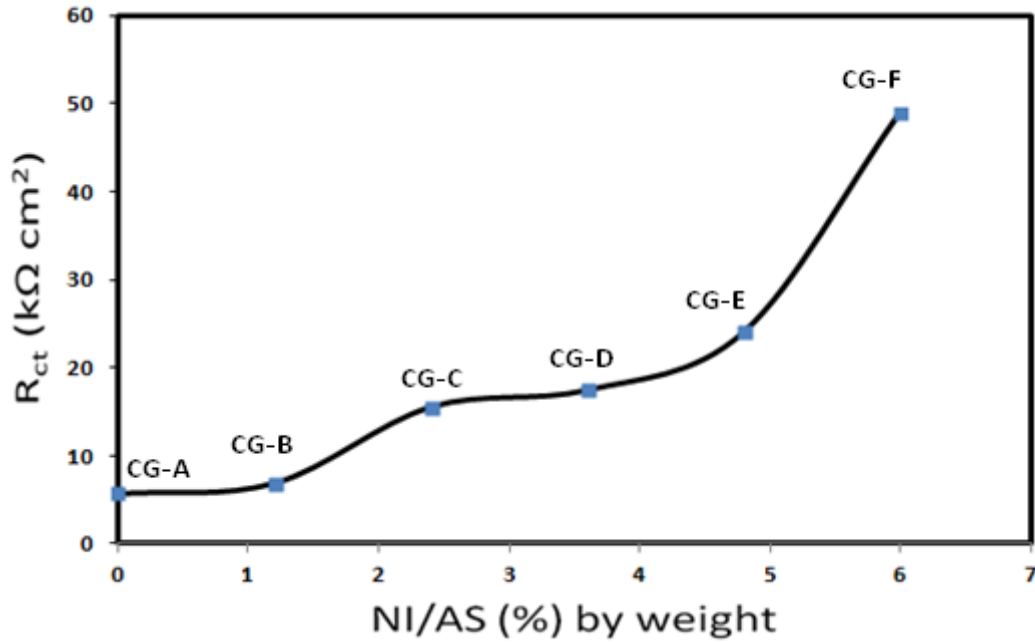CG-F > CG-E > CG-D > CG-C> CG-B> CG-A> Blank carbon steel

Fig 6: Show increase in charge transfer resistance with increasing the added NI/AS modifier (%) by weight in the coating formulation.
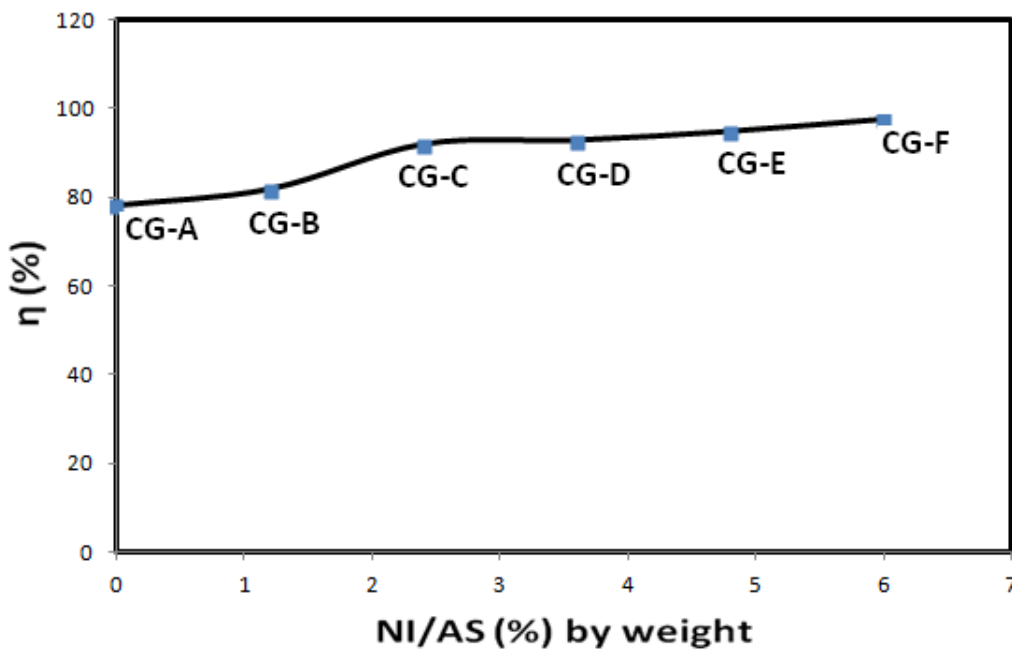

Fig 7: Show increase in the protection efficiency with increasing the added NI/AS modifier (%) by weight in the coating formulation.

This behavior is owing to blocking the voids and pinholes of coating matrix by the lamellar effect of the flaky-like particles of the NI/AS. In case of CG-A coating (unmodified) gave the minimum protection efficiency because the spherical Zn-dust particles permit a clearly-distance between each other (pinholes and voids) during their dispersion through the coating binder in which percolation of aggressive ions, oxygen and water through them has been happened.

Energy dispersive analysis of X-rays (EDX)

EDX investigation was used to survey the protective film formed on the prepared carbon steel surface in oil-wells formation water. The EDX is a semi-quantitative analysis and gives an idea about the composition of the formed protective film. The peak of Fe (detected by the arrow) in the absence and presence of the cold galvanizing coating films gives an idea about the thickness of the protective film formed due to the highly content of dispersed nanocomposite modifier. EDX spectrum of the polished carbon steel sample in **Fig.8a** shows good surface properties, while the spectrum in case of carbon steel sample immersed in formation water was failed in the absence of the cold galvanizing coating film due to the directly external corrosion as shown in **Fig. 8b**. In case of **Fig. 8C**, by application of the CG-C cold galvanizing coating layer on the steel surface, the surface of the carbon steel sample was improved due to formation of the protective film of zinc dust-alkyd interaction but with some voids through the paint layer. The EDX analysis for CG-F coated steel sample shows the minimum level of the Fe band as shown in **Fig. 8d**. This was attributed to the higher concentration of nanocomposite particles in case of CG-F coating film (6% nanocomposite content) in which aligned parallel to the steel surface through the modified alkyd binder producing a shield of the overlapping plates. The well-dispersion of nanocomposite particles through the alkyd resin matrix increased the interface surface interaction between the nanoparticles and the resin matrix in which led to occupying any holidays through the coating film. So, the protective film formed was strongly adherent to the surface, leading to a high degree of inhibition efficiency and made shielding for the iron [24].
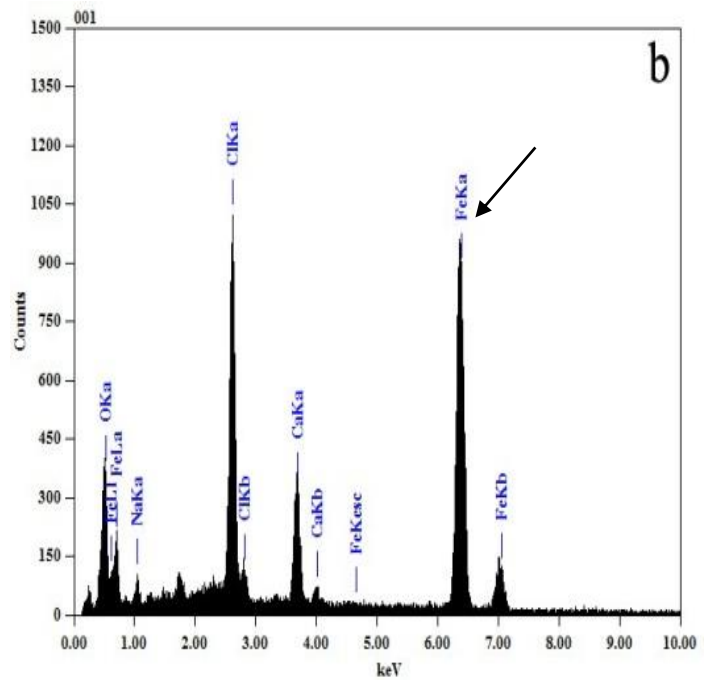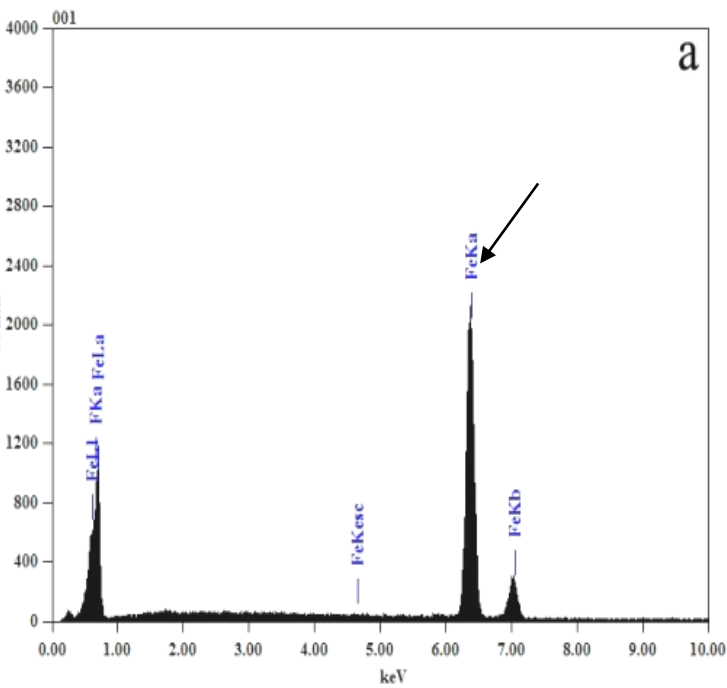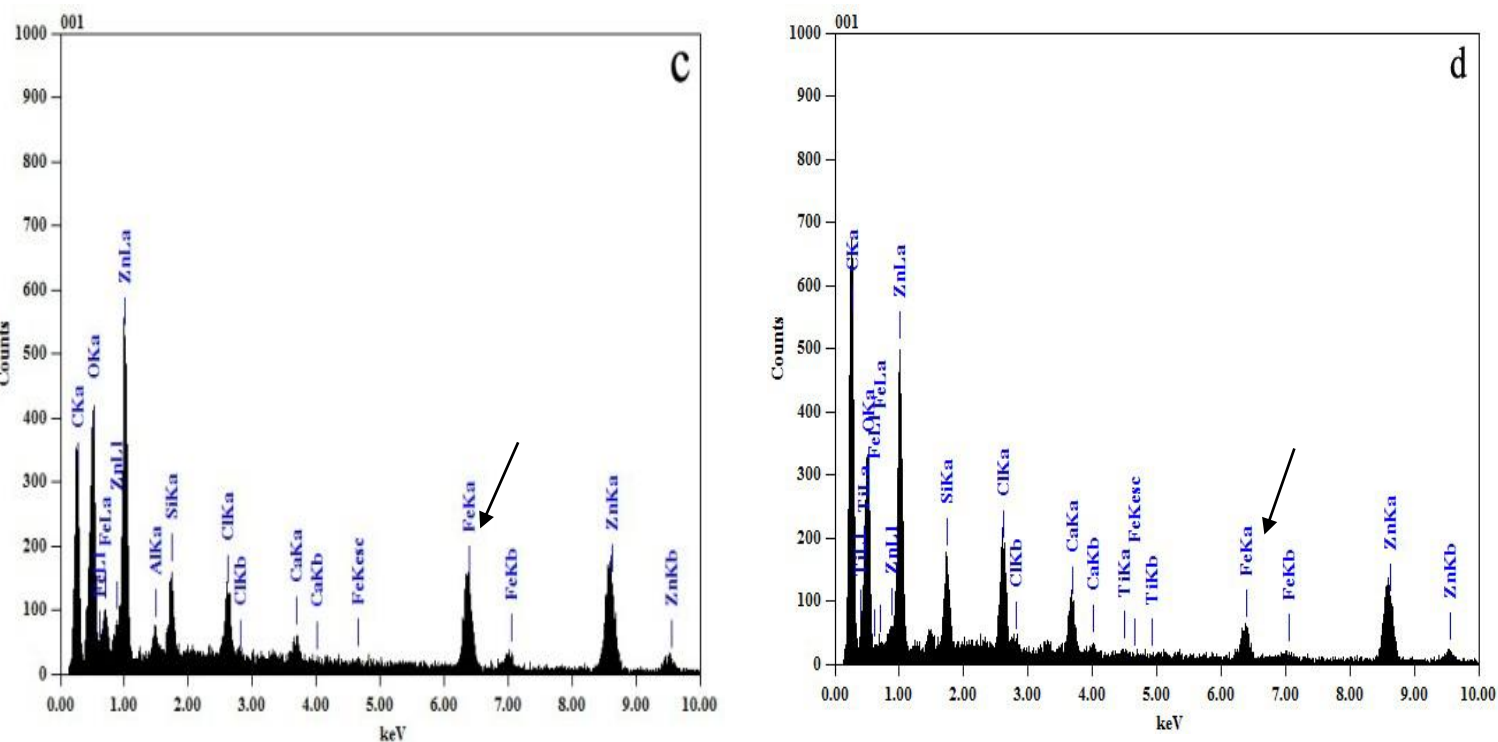
Fig 8: EDX images of (a) abraded steel panel (b) abraded steel panel after immersion in formation water solution for 21 days (c) CG-A coated steel panel after immersion to the same duration (d) CG-F coated steel panel after immersion to the same duration.

CONCLUSIONS

Nanoilmenite/amorphous silica composite (NI/AS) particles were prepared and characterized by TEM and SEM investigations. Different alkyd-based cold galvanizing coating formulations were modified using various uniformly dispersing amounts of the processed NI/AS particles as a modifier to form some nanocomposite coatings. The corrosion protection behavior of treated nanocomposite cold galvanizing coating against untreated conventional one was studied by EIS and EDX techniques. EIS results indicated an increase in the charge transfer resistance (R_{ct}) values and a decrease in the double layer capacitance (Q_{dl}) with increasing the concentration of NI/AS modifier. The formation of good protective film by the NI/AS modified cold galvanizing coatings on the steel surface in formation water solution was confirmed by EDX technique.

REFERENCES

[1] Shi Hongwei, Liu Fuchun, Han En-Hou. *Surface and Coating Technology* 2011; 205(19): 4532-39.
[2] Hare CH. *J. Protective Coatings & Linings* 1998;14: 47-82.
[3] Meroufela A, Touzain S. *Progress in Organic Coatings* 2007;59: 197-205.
[4] Morcillo M, Barajas R, Feliu S, Bastidas JM. *J. Material Science* 1990;25(5): 2441-46.
[5] Pereira D, Scantlebury JD, Ferreira MGS, Almeida ME. *Corrosion Science* 1990; 30(11): 1135-1147.
[6] Wicks ZW, Jones FN, Pappas SP. *Organic Coating: Science and Technology*, 2nd edition: John Wiley & Sons, 1994.
[7] Fadl AM, Al-Sabagh AM, Abdou MI, Migahed MA. *ARE Patent* 27679. 2016.
[8] Ajayan PM, Schadler LS, Braun PV. *Nanocomposite Science and Technology*, Wiley-VCH,. 2003.
[9] Ng CB, Schadler\ LS, Siegel RW. *Nanostructured Materials* 1999;12: 507.
[10] Nq CB, Ash BJ, Schadler LS. *Advanced Composites Letters* 2001;10: 101-11.
[11] Abdou MI, Fadl AM, Al-Sabagh AM, Abuseda HH. *ARE Patent* 2014030455. 2014.
[12] Sattler C, De Oliveira L, Tzschirner M, Machado AEH. *Energy* 2004;29: 835-43.
[13] Hegazy MA, Hefny MM, Badawi AM, Ahmed MY. *Progress in Organic Coatings* 2013;76: 827-34.
[14] Bockris J, Reddy KN. *Modern Electrochemistry*, New York: John Wiley & Sons, 1976.

[15]   Calle LM, MacDowell LG. 5th international symposium on electrochemical impedance spectroscopy, marilleva, 2001.
[16]   Abreu CM, Izquierdo M, Keddam M, Novoa XR, Takenoui H. *Electrochimica Acta* 1996;41: 2405-2415.
[17]   Prabhu RA, Venkatesha TV, Shanbhag AV, Kulkarni GM, Kalkhambkar RG. *Corrosion Science* 2008;50: 3356-62.
[18]   Mathiazhagan A, Joseph Rani. *International Journal of Chemical Engineering and Applications* 2011;2(4): 226.
[19]   Stoynov ZB, Grafov BM, Savova BS, Elkin VV. Electrochemical impedance, Nauka, Moscow, 1991.
[20]   Barsoukov E, Ross Macdonald J. *Impedance Spectroscopy: Theory, Experiment and Applications*, John Wiley& Sons Inc. 2005.
[21]   Simões AM, Fernandes J CS. *Progress in Organic Coatings* 2010;69: 219-24.
[22]   Migahed MA, Al-Sabagh AM, Zaki EG, Mostafa HA, Fouda AS. *International Journal of Electrochemical Science* 2014;9: 7693 - 7711.
[23]   Saliyan VR, Adhikari AV. *Corrosion Science* 2008;50: 55-61.
[24]   Amin MA. *J. Applied Electrochemistry* 2006;36 (2) 215-26.